

Design and characterization of a new pressurized flat panel photobioreactor for microalgae cultivation and CO<sub>2</sub> bio-fixation

*Original*

Design and characterization of a new pressurized flat panel photobioreactor for microalgae cultivation and CO<sub>2</sub> bio-fixation / Carone, Michele; Alpe, Davis; Costantino, Valentina; Derossi, Clara; Occhipinti, Andrea; Zanetti, Mariachiara; Riggio, Vincenzo A. - In: CHEMOSPHERE. - ISSN 0045-6535. - 307:Pt 2(2022), p. 135755.  
[10.1016/j.chemosphere.2022.135755]

*Availability:*

This version is available at: 11583/2971905 since: 2022-10-25T09:52:50Z

*Publisher:*

Elsevier

*Published*

DOI:10.1016/j.chemosphere.2022.135755

*Terms of use:*

This article is made available under terms and conditions as specified in the corresponding bibliographic description in the repository

*Publisher copyright*

Elsevier postprint/Author's Accepted Manuscript

© 2022. This manuscript version is made available under the CC-BY-NC-ND 4.0 license  
<http://creativecommons.org/licenses/by-nc-nd/4.0/>. The final authenticated version is available online at:  
<http://dx.doi.org/10.1016/j.chemosphere.2022.135755>

(Article begins on next page)

1 **Design and characterization of a new pressurized flat panel photobioreactor for**  
2 **microalgae cultivation and CO<sub>2</sub> bio-fixation.**

3 Michele Carone\*<sup>1</sup>, Davis Alpe<sup>2</sup>, Valentina Costantino<sup>1</sup>, Clara Derossi<sup>1</sup>, Andrea  
4 Occhipinti<sup>3</sup>, Mariachiara Zanetti<sup>1</sup>, Vincenzo A. Riggio<sup>1</sup>

5 1: Department of Environment, Land and Infrastructure Engineering, Politecnico di  
6 Torino, Corso Duca degli Abruzzi 24, 10129 Torino, Italy

7

8 2: Photo B-Otic S.r.l., Via Paolo Veronese 202, 10148 Torino, Italy

9

10 3: Abel Nutraceuticals S.r.l., Via Paolo Veronese 202, 10148 Torino, Italy

11 \* Correspondence to Michele Carone at [michele.carone@polito.it](mailto:michele.carone@polito.it)

12 **Abstract**

13 Microalgae-based biorefinery processes are gaining particular importance as a  
14 biotechnological tool for direct carbon dioxide fixation and production of high-quality  
15 biomass and energy feedstock for different industrial markets. However, despite the many  
16 technological advances in photobioreactor designs and operations, microalgae cultivation  
17 is still limited due to the low yields achieved in open systems and to the high investment  
18 and operation costs of closed photobioreactors. In this work, a new alveolar flat panel  
19 photobioreactor was designed and characterized with the aim of achieving high  
20 microalgae productivities and CO<sub>2</sub> bio-fixation rates. Moreover, the energy efficiency of  
21 the employed pump-assisted hydraulic circuit was evaluated. The 1.3 cm thick alveolar  
22 flat-panels enhance the light utilization, whereas the hydraulic design of the  
23 photobioreactor aims to improve the global CO<sub>2</sub> gas-liquid mass transfer coefficient  
24 ( $k_{LaCO_2}$ ). The mixing time, liquid flow velocity, and  $k_{LaCO_2}$  as well as the uniformity  
25 matrix of the artificial lighting source were experimentally calculated. The performance  
26 of the system was tested by cultivating the green microalga *Acutodesmus obliquus*. A  
27 volumetric biomass concentration equal to 1.9 g L<sup>-1</sup> was achieved after 7 days under

28 controlled indoor cultivation conditions with a CO<sub>2</sub> bio-fixation efficiency of 64 % of  
29 total injected CO<sub>2</sub>. The (gross) energy consumption related to substrate handling was  
30 estimated to be between 27 and 46 Wh m<sup>-3</sup>, without any cost associated to CO<sub>2</sub> injection  
31 and O<sub>2</sub> degassing. The data suggest that this pilot-scale cultivation system may constitute  
32 a relevant technology in the development of microalgae-based industrial scenario for CO<sub>2</sub>  
33 mitigation and biomass production.

#### 34 **Keywords**

35 Flat panel photobioreactor, CO<sub>2</sub> mass transfer coefficient, CO<sub>2</sub> bio-fixation efficiency,  
36 Hydrodynamic characterization, *Acutodesmus obliquus*.

37

#### 38 **1. Introduction**

39 Since the 20th century, the concentration of greenhouse gases in the atmosphere  
40 continued to increase as result of anthropogenic activities related to the use of fossil fuels,  
41 deforestation, and agricultural activities. The annual global average carbon dioxide  
42 concentration at Earth's surface in 2020 has reached  $412.5 \pm 0.1$  ppm, the highest value  
43 in modern atmospheric records, increasing by  $2.5 \pm 0.1$  ppm from 2019, a value  
44 comparable to the average rate of increase during the last decade (Blunden and Boyer,  
45 2021). Therefore, the development of renewable and clean technologies is needed to  
46 sustain a considerable fraction of the global economy and to reduce the impact of human  
47 activities. In parallel, major efforts are needed to improve CO<sub>2</sub> Capture and Utilization  
48 (CCU) technologies that can effectively reduce carbon dioxide emissions mainly from  
49 power plants and different industrial processes.

50 In this context, microalgae-based refinery concepts have gained importance over the  
51 last few decades. Microalgae are considered promising biochemical factories and  
52 excellent CO<sub>2</sub> fixers (Brown and Zeiler, 1993). Their simple cellular structure, large

53 surface-to-volume ratio, and aquatic lifestyle allow these organisms an easy access to  
54 water, CO<sub>2</sub> and other nutrients, and thus a more efficient conversion of solar energy into  
55 chemical energy, showing 10-50 higher CO<sub>2</sub> fixation rates than land plants (Carlsson et  
56 al., 2007; Goli et al., 2016; Rosenberg et al., 2011). Moreover, compared to higher plants,  
57 microalgae also show faster growth rates and their cultivation does not compete for arable  
58 lands (Greenwell et al., 2010; Khan et al., 2009). As a result of CO<sub>2</sub> fixation, microalgae  
59 accumulate significant amounts of carbohydrates, proteins, lipids, and other valuable  
60 compounds, such as pigments and vitamins. Hence, microalgal biomass is considered a  
61 promising energy feedstock with multifaceted applications in the production of dietary  
62 supplements, cosmetics, food and animal feed and biofuels (Cheah et al., 2015; Francisco  
63 et al., 2010; Gimpel et al., 2015; Vanthoor-Koopmans et al., 2013). Algal cultivation  
64 technologies are traditionally classified as open or closed systems (photobioreactors,  
65 PBRs). Open cultivation systems (*e.g.*, artificial ponds, raceways, thin layer) produce  
66 algal biomass at lower costs thanks to their lower investment and management costs in  
67 terms of Capital Expenditure (CapEx) and Operating Expense (OpEx) (Benemann, 2013).  
68 The open raceway pond is currently the most frequently used and cheapest cultivation  
69 system for commercial production of microalgae (Acién et al., 2017). Despite this, the  
70 open pond technology is limited by several disadvantages such as low biomass  
71 productivities, mainly related to poor mixing, low CO<sub>2</sub> mass transfer, high risk of  
72 biological and chemical contamination and high consumption of water. Moreover, its  
73 dependence on climatic conditions limits its application to tropical and subtropical  
74 regions (Chini Zittelli et al., 2013; Pandey et al., 2014; Tredici et al., 2010). On the other  
75 hand, closed photobioreactors allow precise control of the operating conditions and show  
76 higher biomass productivities. The confined space limits contaminations and assures  
77 higher biomass quality, but requires higher CapEx and OpEx (Adesanya et al., 2014;  
78 Norsker et al., 2011). Currently, tubular photobioreactors are the most common closed

79 system configurations for industrial-scale microalgae cultivation, mainly related to high-  
80 value applications (Acién et al., 2017; Chini Zittelli et al., 2013; Torzillo and Zittelli, 2015).  
81 However, all types of closed systems present major constraints in the process scale-up,  
82 mainly due to the difficulty in increasing the sizes of PBRs while keeping optimal culture  
83 and hydrodynamic parameters. The choice of the circulating device and design of the  
84 PBR influences important operating parameters such as mixing time, turbulence degree,  
85 O<sub>2</sub> build-up, and CO<sub>2</sub> supply, thus impacting on both the overall performance of the  
86 process (Torzillo et al., 2003) and the final cost. An extensive comparison of the strengths  
87 and limitations of the different cultivation systems, together with the importance of  
88 illumination and hydrodynamic parameters, has been thoroughly analysed in several  
89 reviews (Acién et al., 2017; Carvalho et al., 2006; De Vree et al., 2015; Torzillo and Zittelli,  
90 2015; Tredici et al., 2010; Yadav and Sen, 2017). It is important to note that, although many  
91 PBRs and open system setups have been proposed at laboratory and industrial levels,  
92 there is no optimal design for all applications. Moreover, the overall negative energy  
93 balance of the processes still poses limitations in the scale-up of microalgal culture  
94 technologies, making them profitable only for applications with high added value goods  
95 such as dietary supplement and cosmetic raw materials (Acién et al., 2012; Slade and  
96 Bauen, 2013; Tredici et al., 2015). Recently, several studies have focused on the  
97 development of many simulation approaches coupling computational fluid dynamics,  
98 mass transport phenomena and microbial growth kinetics, to identify the best conditions  
99 to maximize microalgae productivity (del Rio-Chanona et al., 2019; Solimeno et al.,  
100 2017; Tan et al., 2020; Vasile et al., 2021; Weise et al., 2019). Likewise, several new  
101 design of open, closed, and hybrid PBRs setups based on different hydrodynamics, mass  
102 transfer mechanisms and illumination strategies have been proposed to improve the  
103 global cultivation efficiency and the scale-up feasibility (Chen et al., 2016; Chiaramonti et  
104 al., 2013; Cuaresma et al., 2009; Estrada-Graf et al., 2020; Li et al., 2014; López-Rosales et

105 al., 2019; Massart et al., 2014; Reyna-Velarde et al., 2010; Rodolfi et al., 2009; Sierra et al.,  
106 2008; Tan et al., 2020; Tredici et al., 2015; Yadav et al., 2015). Particularly, more attention  
107 was given to flat panel PBRs due to the high photosynthetic efficiencies that can be  
108 reached (Jorquera et al., 2010). However, currently employed flat panel PBRs still present  
109 some limitations mainly due to the low mixing efficiency, being the air bubbled mainly  
110 directly from the bottom of the panels, which brings to high energy costs and can lead to  
111 the occurrence of serious biofouling (Sierra et al., 2008; Tredici et al., 2015). Moreover,  
112 the use of compressed air for mixing constitutes a major part of the PBR energy  
113 consumption. Indeed, the power supply associated to air compression is function of the  
114 type of compressor, gas pressure, type of blower, and the aeration rate (Norsker et al.,  
115 2012). Centrifugal pumps, which are considerably more efficient than air compressors,  
116 have been mainly employed in tubular PBRs, although the concern for cell shear damage  
117 has led more frequently to the use of air-lift pumps. Nevertheless, as pointed out by  
118 Norsker and co-authors, the use of centrifugal pumps would be not recommended only  
119 for the cultivation of very shear sensitive algae (Norsker et al., 2011). To our knowledge,  
120 no literature reports are present concerning pilot-scale flat panel PBRs with a centrifugal  
121 pump. In this research, it is presented the design and characterization of a novel alveolar  
122 flat panel photobioreactor with a pump-assisted hydraulic circuit, that constrains  
123 microalgae to flow inside a positive-pressurized serpentine directly exposed to the  
124 artificial light source. The system has been realized to maximize the distribution of light  
125 through the microalgae culture as the width of the flat panels is equal to 1.3 cm. The main  
126 purpose of this work was to assess the hydrodynamic and cultivation performances of the  
127 proposed PBR. The results will help to improve the actual proposed technology and to  
128 evaluate its possible use in an industrial scenario, in which the application of energy-  
129 efficient technologies is nowadays a priority.

130 Therefore, the hydraulic, lighting and energetic behaviour of the new flat-panel PBR  
131 were investigated through the experimental characterization of the hydraulic flow, mixing  
132 time, CO<sub>2</sub> gas-liquid mass transfer coefficient, and irradiance matrix. The biological  
133 performances of this new prototype were tested by cultivating the green microalga  
134 *Acutodesmus obliquus*.

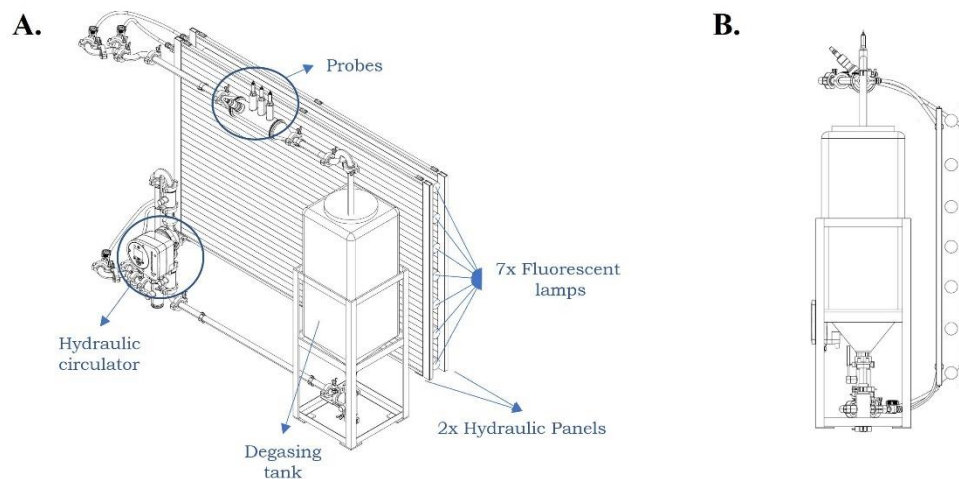
135

## 136 **2. Materials and Methods**

### 137 **2.1 The flat panel photobioreactor**

138 The photobioreactor used in this research was kindly provided by Arcobaleno  
139 Cooperativa Sociale (Turin, Italy), the patent holder of the PBR (EP2830413A1). A  
140 representative scheme of the PBR is reported in Figure 1A. Briefly, it is composed by  
141 two interconnected units: a photostage loop and a mixing tank. The photostage loop  
142 consists of two parallel alveolar flat panels illuminated by an interposed array of seven  
143 fluorescent lamps (58W, OSRAM, Germany). The alveolar flat panels are made of  
144 transparent polycarbonate with a light exposed surface area of 1.5 m<sup>2</sup> each and an  
145 internal path of 13 mm. Each panel is partitioned into 28 internal channels (alveoli) for  
146 a total length of the illuminated path of about 40 m and total volume of about 17 L. The  
147 mixing tank is made up with a darkened HDPE (High density polyethylene) material  
148 with a total volume of 50 L. Its truncated-cone shape has been designed to minimize  
149 biomass sedimentation (Fig. 1B). The tank is equipped on its top of a hydraulic inlet  
150 and a removable lock cap. A hydraulic circulator (ALPHA1 L - 45W, Grundfos,  
151 Denmark) is connected at the bottom of the mixing tank and upstream of the photostage  
152 loop. The hydraulic circulator drives the liquid flow into both flat panels, from the  
153 bottom to the top. Moreover, the hydraulic circulator allows to manually set up three  
154 different factory-defined liquid flow rates operating with constant performance curves.  
155 Gas inlet coming from a food grade CO<sub>2</sub> tank is located between the bottom of mixing

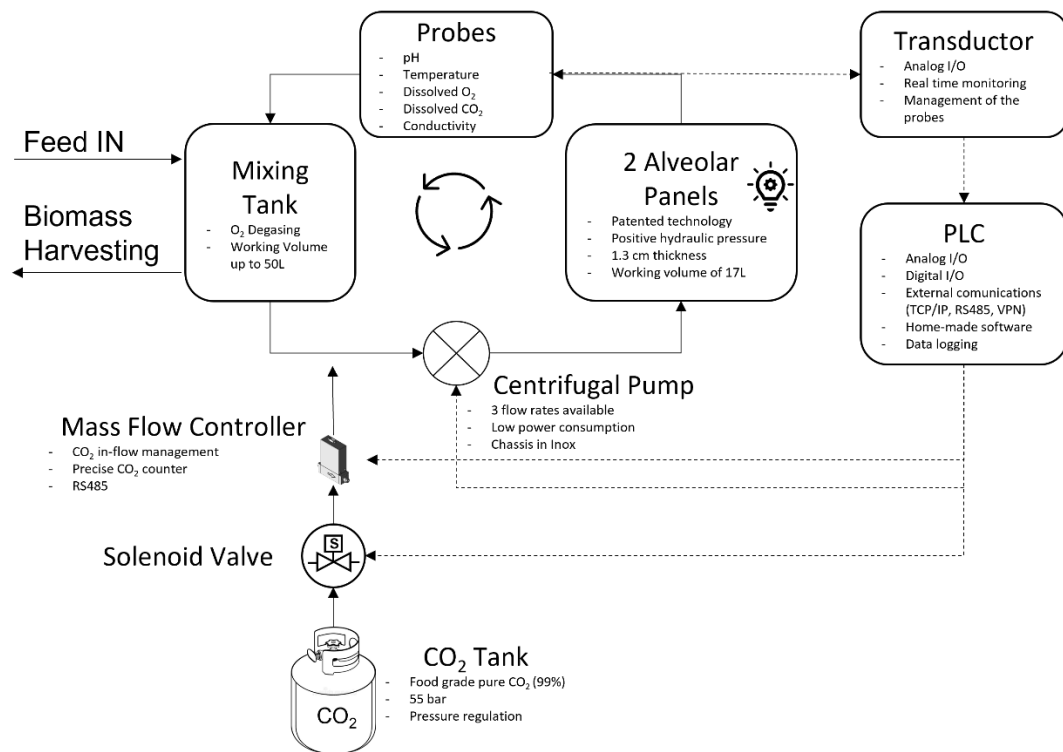
156 tank and the hydraulic circulator. This configuration maximizes gas dissolution in the  
157 liquid phase thanks to the turbulence generated by the circulation system. CO<sub>2</sub> flow  
158 rates are finely regulated by a thermal flow meter (Red-y smart controller GSC, Vögtlin  
159 Instruments GmbH Switzerland), whereas temperature/pH, conductivity, dissolved  
160 oxygen, and carbon dioxide are constantly monitored by a InPro 325Xi pH electrodes,  
161 Four-electrode conductivity sensor, InPro 6000 Optical O<sub>2</sub> sensor and a InPro 5000i  
162 CO<sub>2</sub> sensor (Mettler-Toledo®, USA), respectively. The probes are located at the output  
163 of the flat panels. The PBR is equipped with a Mettler-Toledo® multi-parameter  
164 transducer M800 and the signals from the sensors are transmitted to a Programmable  
165 Logical Controller (PLC, Unitronics, Israel) through industrial standard analogic signal  
166 protocol (4-20 mA). The PLC controls a dedicated solenoid valve for the CO<sub>2</sub> injection,  
167 allowing the regulation of the CO<sub>2</sub> flow based on pH or carbon dioxide concentration  
168 threshold, according to the experimental setup. A schematic overview of the whole PBR  
169 working process is reported in Figure 2.



170  
171 **Figure 1:** Schematic representation of the flat panel photobioreactor. A) 3D isometric  
172 view of the whole PBR. B) Schematic view of the mixing tank.

173





174

175 **Figure 2:** Schematic process diagram of the flat panel photobioreactor.

176

## 177 2.2 Microalgae and cultivation conditions

178 *Acutodesmus obliquus* strain 276-3b, formally *Scenedesmus obliquus* (Turpin) Kützing,  
 179 was obtained from the SAG Culture Collection of Algae (Göttingen, Germany). The  
 180 inoculum preparation was carried out in batch mode and axenic conditions in 2 L  
 181 disposable culture chambers by using a 1.5 L volume of sterile BG-11 medium (Stanier  
 182 et al., 1971). The cultures were maintained at constant temperature ( $23^{\circ}\text{C} \pm 2$ ), pH 7.00-  
 183 7.50, and under constant (24/24 h of illumination) artificial illumination ( $120 \mu\text{mol m}^{-2} \text{s}^{-1}$ )  
 184 <sup>1)</sup> by fluorescence tubes (Osram, Germany). Aeration and mixing of the cells were  
 185 guaranteed by flowing air at the bottom of the chambers. The microalgal cells were used  
 186 to inoculate the flat panel photobioreactor when they just reached the stationary phase.  
 187 The PBR was inoculated with BG-11 medium and microalgae cells for a total volume of  
 188 60 L, corresponding to a surface area-to-volume ratio ( $S_f/V$ ) of  $50 \text{ m}^{-1}$ , and an initial cell  
 189 concentration of  $0.25 \text{ g L}^{-1}$  of dry weight. Each experiment in the PBR was conducted in

190 batch mode for 7 days. The injection of CO<sub>2</sub> was carried out with a flow rate of 0.12 L  
191 min<sup>-1</sup>, keeping constant the CO<sub>2</sub> concentration threshold in the PBR at 25 mg L<sup>-1</sup> using  
192 the combination of solenoid valve and mass flow meter.

193

### 194 **2.3 Biomass concentration measurements**

195 Microalgae growth was gravimetrically quantified as dry biomass concentration as  
196 previously reported (Perin et al., 2017). Briefly, 10-20 mL of microalgae culture was  
197 filtered using pre-weighted 1.5 µm pore size glass fibre filters (Hahnemühle, Germany).  
198 The filters were then dried using a thermobalance (MLS-N, Kern, Germany) until stable  
199 weight, and then weighted with an analytical balance (Kern, Germany).

200 The biomass volumetric productivity ( $P_x$ ) was then calculated as [Eq. 1]:

$$P_x = \frac{X_t - X_0}{t - t_0} \quad (1)$$

201 where  $X_t$  is the biomass concentration [g L<sup>-1</sup>] at time  $t$  [d], and  $X_0$  is the biomass  
202 concentration [g L<sup>-1</sup>] at time  $t_0$  [d].

203

### 204 **2.4 Hydraulic flow determination**

205 The hydraulic flow rate of the hydraulic circulator was measured using an  
206 electromagnetic flow meter (FD-Q20C. Keyence, Japan). All measurements were carried  
207 out by placing the flow meter at the outlet of the hydraulic panels.

208

### 209 **2.5 CO<sub>2</sub> mass transfer coefficient ( $k_{LaCO_2}$ )**

210 In order to estimate gas-liquid transfer efficiencies of the photobioreactor, the  $k_{LaCO_2}$   
211 was measured using 60L of distilled water (without microalgal cells) to avoid  
212 interferences of biological activity. The test was conducted at room temperature and  
213 atmospheric pressure (25 ± 2°C and 101.325 Pa).

214 The tests were conducted by blowing a constant and continuous flow rate of CO<sub>2</sub> inside  
215 the PBR and monitoring, through the CO<sub>2</sub> probe, the carbon dioxide concentration over  
216 time. Different carbon dioxide flow rates were tested at different hydraulic circulator  
217 powers (different hydraulic flow rate). As indicated in paragraph [2.1], the PBR employs  
218 a circulation system that allows to choose between three different levels of power flows  
219 corresponding to three different liquid rates. For each circulation level, the  $k_La$  value was  
220 identified for different carbon dioxide flow rates.

221 The  $k_La_{CO_2}$  parameter was determined using the following equation [Eq. 2](Sierra et  
222 al., 2008):

$$\frac{dC}{dt} = k_La * (C^* - C) \quad (2)$$

223

224 integration for  $C = C_0$  at  $t = 0$  lead to [Eq. 3]:

$$\ln\left(\frac{C^* - C}{C^* - C_0}\right) = -k_La * t \quad (3)$$

225

226 where  $C_0$  is the initial CO<sub>2</sub> concentration [mg L<sup>-1</sup>],  $C$  is the dissolved CO<sub>2</sub> concentration  
227 [mg L<sup>-1</sup>] at time  $t$ ,  $C^*$  is the CO<sub>2</sub> saturation concentration in water [mg L<sup>-1</sup>] and  $t$  is time  
228 [min]. Since dissolved carbon dioxide is in equilibrium with carbonate and bicarbonate  
229 species, to determine the exact concentration of carbon dissolved into the aqueous phase  
230 the relevant equilibrium and corresponding equilibrium constants were calculated as  
231 previously reported (Chen et al., 2016).

232

## 233 **2.6 CO<sub>2</sub> fixation yield**

234 The CO<sub>2</sub> fixation yield ( $\eta_{CO_2}$ ) expresses the CO<sub>2</sub> bio-fixation rate of the culture in terms  
235 of percentage (Lim et al., 2021). It is calculated as the ratio between the kilograms of  
236 carbon accumulated within the algal biomass at the end of the cultivation and the kg of

237 carbon supplied to the microalgae through the injection of CO<sub>2</sub> at a known flow rate [Eq.  
238 4], as previously reported (Lim et al., 2021).

$$\eta_{CO_2} = \frac{W_{C \text{ biomass}}}{W_{C \text{ in}}} * 100 \quad (4)$$

239

240 With  $W_{C \text{ biomass}}$  and  $W_{C \text{ in}}$  deriving respectively from [Eq. 5] and [Eq. 6]:

$$W_{C \text{ biomass}} = W_{\text{biomass}} * C_{C \text{ biomass}} \quad (5)$$

$$W_{C \text{ in}} = (W_{CO_2 \text{ in}} - W_{CO_2 \text{ water}}) * (M_C / M_{CO_2}) \quad (6)$$

241

242 Where  $W_{C \text{ biomass}}$  is the kg of carbon accumulated in the biomass;  $W_{\text{biomass}}$  the kg of  
243 biomass obtained during the cultivation;  $C_{C \text{ biomass}}$  is the fraction of carbon within the cells  
244 obtained through experimental elemental analysis of *A. obliquus*;  $W_{C \text{ in}}$  is the kg of carbon  
245 injected into the PBR as CO<sub>2</sub> flow;  $W_{CO_2 \text{ in}}$  is the total kg of CO<sub>2</sub> injected;  $W_{CO_2 \text{ water}}$  is the  
246 kg of CO<sub>2</sub> dissolved in water at the end of the batch;  $M_C$  and  $M_{CO_2}$  represent respectively  
247 the molar mass of carbon (12 g mol<sup>-1</sup>) and carbon dioxide (44 g mol<sup>-1</sup>).

248

## 249 **2.7 Mixing time**

250 The mixing time [ $t_m$ ] is defined as the time required to attain a given uniformity close  
251 to the fully mixed state after the injection of a tracer (Yang and Mao, 2014) and it was  
252 evaluated by a pH tracing test. To estimate the mixing time of the photobioreactor, the  
253 experiments were performed using 60 L of distilled water (without microalgal cells) to  
254 avoid interferences of biological activity. Diluted hydrochloric acid (5 mL HCl; with a  
255 final concentration in the PBR of 10<sup>-3</sup> M) was poured into the mixing tank of the  
256 photobioreactor, and the pH was recorded every minute by the pH probe located at the

257 output of the flat panels. The  $t_m$  was determined as the time required to reach the 95% of  
258 complete homogeneity after the injection of the HCl solution (Chisti, 1989).

259

## 260 **2.8 Energetic measurements**

261 The energy consumption of the PBR main components (hydraulic circulator and  
262 lighting system) was measured using a digital multimeter (Siglent SDM3065X-SC,  
263 Germany). Voltage and current intensity measured for each unit were used to calculate  
264 the power input expressed in Watt [W]. These data, together with the hydraulic flow  
265 measurements, were further computed to evaluate the net energy consumption for the  
266 fluid handling as Wh m<sup>-3</sup>.

267

## 268 **2.9 Radiance matrix**

269 The PBR was illuminated by an artificial lighting system based on an array of seven  
270 fluorescent tubes interposed between the two flat panels. To evaluate the uniformity of  
271 incident light on both exposed surfaces of the panels, the light intensity was determined  
272 by a PAR spectroradiometer (PLA 20, Everfine, China). A matrix array was imposed on  
273 the artificial lighting system to fix and homogeneously distribute the sampling points  
274 along the radiant surface. The data obtained from the measurements were interpolated  
275 using the software Matlab<sup>®</sup> to create the pattern of light intensity for the whole exposed  
276 panel surface.

277 The light uniformity coefficient was calculated using the following equation:

$$U_I = \frac{I_{min}}{I_{mean}} \times 100 \quad (7)$$

278

279 where  $U_I$  is the light uniformity coefficient [%],  $I_{min}$  is the minimum value of light  
280 intensity [ $\mu\text{mol m}^{-2} \text{s}^{-1}$ ] and  $I_{mean}$  is the mean value of light intensity [ $\mu\text{mol m}^{-2} \text{s}^{-1}$ ].

281 **3. Results and discussion**

282 **3.1 Hydrodynamics flow description**

283 This study has described, for the first time in literature, the hydrodynamics, mass  
284 transfer and mixing time parameters of an innovative and patented flat panel  
285 photobioreactor. The experimental characterization of biological performance parameters  
286 has been also reported. Key hydrodynamic parameters have been explored in order to  
287 compare the pump-assisted setup of the cultivation system here reported to traditional flat  
288 panel photobioreactors. In the latter, mixing and liquid flow is typically achieved by air  
289 bubbling or through an external airlift system. Whereas the hydrodynamics of the  
290 described PBR is function of the pump-driven culture flow, and thus is linked to the gross  
291 power of the hydraulic circulator. Therefore, the hydrodynamics characterization of the  
292 reactor included the measurements, at the three default pump setups and at various CO<sub>2</sub>  
293 injection rates, of the different liquid flow rates and the effects on the mixing time and  
294 the CO<sub>2</sub> volumetric mass transfer coefficient ( $k_{LaCO_2}$ ).

295 The hydraulic flow rates calculated using the available standard setups on the circulator  
296 system (hereafter named level I, II, III), and their variations at increasing flow of injected  
297 CO<sub>2</sub> gas were measured. As shown in Table 1, the experimental results showed that,  
298 without any gas injection, the hydraulic flow varies greatly from 4 L min<sup>-1</sup> for the lower  
299 configuration of the circulator to values of 14 and 18 L min<sup>-1</sup> for level II and level III,  
300 respectively. The calculated liquid flow velocity ( $U_L$ ) within the alveoli is 0.17, 0.60 and  
301 0.77 m s<sup>-1</sup> at level I, II and III, respectively.

302

303

304

305

306 **Table 1:** Variation of hydraulic flow rates according to the manually chosen level of the  
 307 hydraulic circulator and the CO<sub>2</sub> flow injection. Liquid flow rates for the higher levels of  
 308 the circulation system, at low CO<sub>2</sub> flow rates, were not measured assuming a negligible  
 309 reduction of the rates according to the data for level I. Liquid flow rates (L min<sup>-1</sup>) are  
 310 shown as the average of three replicates ± standard deviation.  $U_L$  = liquid flow velocity  
 311 (m s<sup>-1</sup>).

<b>Liquid flow rate [L min<sup>-1</sup>]</b>			
<b>CO<sub>2</sub> flow rate [NL min<sup>-1</sup>]</b>	<b>Circulator level I <math>U_L = 0.17 \text{ m s}^{-1}</math></b>	<b>Circulator level II <math>U_L = 0.60 \text{ m s}^{-1}</math></b>	<b>Circulator level III <math>U_L = 0.77 \text{ m s}^{-1}</math></b>
<b>None</b>	4.05 ± 0.03 (100%)	14.11 ± 0.15 (100%)	18.10 ± 0.33 (100%)
<b>0.06</b>	3.66 ± 0.11 (90.4%)	n.d.	n.d.
<b>0.12</b>	3.69 ± 0.09 (91.1%)	n.d.	n.d.
<b>0.48</b>	3.58 ± 0.02 (88.4%)	13.52 ± 0.31 (95.8%)	n.d.
<b>0.60</b>	3.62 ± 0.05 (89.4%)	11.23 ± 0.61 (79.6%)	n.d.
<b>0.84</b>	n.d.	8.61 ± 0.09 (61%)	18 ± 0.05 (99.4%)
<b>1.08</b>	n.d.	n.d.	16.95 ± 0.56 (93.6%)

312  
 313 Since the CO<sub>2</sub> is injected immediately upstream the circulator, the hydraulic flow is  
 314 affected by the gas flow, and it is reduced as the gas flow rate increases. This is mostly  
 315 evident at the level II of the circulator. Gas flow rates above 0.48 NL min<sup>-1</sup> reduce the  
 316 hydraulic flow rate to values below the 90% of the hydraulic load without CO<sub>2</sub> injection.  
 317 On the contrary, the liquid flow rate at level III (18 L min<sup>-1</sup>) is not significantly reduced  
 318 by even higher CO<sub>2</sub> rates. Whereas no significant reductions in the liquid flow occur at  
 319 the lower configuration of the circulator (level I). In the latter case, the low liquid flow (4  
 320 L min<sup>-1</sup>) could favor a gas leak toward the tank rather than being swallowed up by the  
 321 circulator and dissolved within the bulk flow to the hydraulic panels.

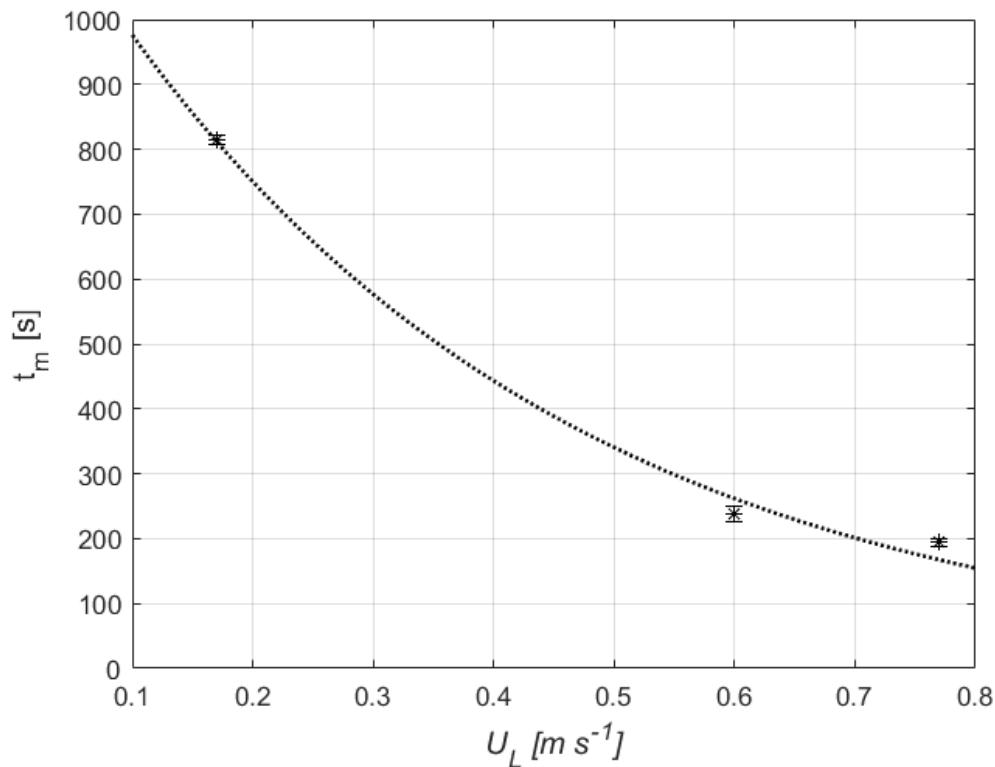
### 322 3.2 Mixing characterization

323 The mixing time ( $t_m$ ) has been calculated at the three nominal liquid velocities, without  
324 CO<sub>2</sub> gas injection, to identify the relationship between  $t_m$  and  $U_L$  in the characterized  
325 cultivation system. The data showed that, by increasing the liquid velocity from 0.17 m  
326 s<sup>-1</sup> (level I) to 0.60 m s<sup>-1</sup> (level II), the mixing time decreases from 814 s to 246 s. Whereas  
327 above  $U_L = 0.60$  m s<sup>-1</sup> the slope of the curve decreases, and the  $t_m$  is not consistently  
328 reduced (194 s) (Fig. 3). The best fitting curve of the experimental data has an exponential  
329 trend (Fig. 3).

330 The computed energy consumption for the fluid handling at the three different liquid  
331 velocities was calculated to be 46, 27 and 38 Wh m<sup>-3</sup>, respectively. Therefore, the reported  
332 power consumption values suggest that working at  $U_L$  values above 0.60 m s<sup>-1</sup>, the  
333 inflexion point of  $t_m$  and  $U_L$  curve, is energetically disadvantageous since mixing time  
334 remains comparable with the one measured at 0.60 m s<sup>-1</sup> (level II).

335 The reactor hydrodynamic behavior of other flat panel PBRs described in literature is  
336 based on different engineering solutions that affect hydrodynamic characteristics  
337 (Massart et al., 2014; Sierra et al., 2008). The authors reported the trend of mixing time in  
338 correlation with the gas velocity which drives the liquid handling. In the PBR prototype  
339 here described, the photosynthetic loop can be assimilated mainly to a plug flow reactor,  
340 although a continued stirred situation may be assumed since the estimated Reynolds  
341 number within the alveoli ( $Re \sim 10,000$ ) indicates a turbulent state. Meanwhile, the  
342 mixing tank can be described as a CSTR (Continued Stirred Tank Reactor). Despite the  
343 different liquid handling solution, adopted in this study, with respect to the reported  
344 literature, the  $t_m$  values measured at 0.60 (level II) and 0.77 m s<sup>-1</sup> (level III) fall into the  
345 ranges of mixing times reported in the above-mentioned works (Massart et al., 2014; Sierra  
346 et al., 2008).





347

348 **Figure 3:** Influence of liquid flow velocity on mixing time. Data are shown as the  
 349 average of three replicates  $\pm$  standard deviation. Dotted line represents the exponential  
 350 fitting ( $R^2 = 0.9946$ ) obtained with the software Matlab®.

351

### 352 3.3 CO<sub>2</sub> mass transfer

353 Carbon dioxide uptake is one of the main target of microalgae cultivation technologies  
 354 exploitation, therefore the CO<sub>2</sub> mass transfer coefficient ( $k_{LA}CO_2$ ) in the new PBR  
 355 prototype was investigated. As described in section [2.1], CO<sub>2</sub> is directly injected  
 356 upstream of the circulation system and the bubbles are swallowed up and broken by the  
 357 circulator to smaller sizes. Moreover, the gas circulates within the fluid in the flat panels  
 358 with a CO<sub>2</sub> bubbles residence time that is linked to the total length of the alveoli in the  
 359 photostage loop (around 40 m).

360 The injection of CO<sub>2</sub> causes a reduction in the hydraulic flow rate since the gas flow  
 361 interferes with the liquid handling of circulator, as discussed in section [3.1]. Therefore,  
 362  $k_{LA}$  values were not measured for the CO<sub>2</sub> flow rates reducing the hydraulic flow below

363 the 90% of nominal value (Table 1) and the results are reported in Table 2. As expected,  
364 the data showed a significant increase of  $k_{La}CO_2$  values from  $1.21 \cdot 10^{-5}$  to  $2.99 \cdot 10^{-4} s^{-1}$   
365 along with the increase of the  $CO_2$  flow injected for each hydraulic flow. The lowest  $k_{La}$   
366 values, meaning a more efficient  $CO_2$  mass transfer, were achieved at the lowest  $CO_2$   
367 flows (0.06 and 0.12 NL  $min^{-1}$ ) for all the circulator flow rates. However, at the circulator  
368 level I (0.17 m  $s^{-1}$ ) the measurements of  $k_{La}CO_2$  may be affected by a gas leak toward the  
369 mixing tank. Furthermore, such low liquid flow velocity determines the longest mixing  
370 time of the PBR system (section [3.2]), which could affect the microalgae growth *e.g.*, by  
371 favoring the sedimentation of biomass. The decrease of  $k_{La}CO_2$  at level III, with respect  
372 to level II, can be justified by the higher speed of the pump that favors the breaking and  
373 mixing of  $CO_2$  gaseous bubbles. However, circulator level III (0.77 m  $s^{-1}$ ) did not show a  
374 relevant improvement of hydraulic and mass transfer performances and it has a higher  
375 energy consumption with respect to circulator level II (section [3.2]). Therefore, the  
376 circulator and  $CO_2$  flow setups showing the best performances in term of hydrodynamics,  
377  $CO_2$  mass transfer and energy consumption were identified to be circulator level II with  
378 the injection of  $CO_2$  flow rates of 0.06 and 0.12 NL  $min^{-1}$ .

379 In the presented prototype, being the system's hydrodynamics based on a mechanical  
380 circulation of the liquid, there is no need to inject air to support the movement of the  
381 liquid culture and guarantee a certain degree of mixing and gas transfers. Thus, it is  
382 possible to inject only pure low  $CO_2$  flow rates achieving a high solubilization in the  
383 photostage loop. In this way,  $CO_2$  losses in atmosphere are limited, and the only cost to  
384 obtain an efficient mixing and gas transfer is the one associated to the hydraulic circulator,  
385 as in real scale application pure  $CO_2$  comes already pressurized by previous industrial  
386 stages. In literature, few examples of  $k_{La}CO_2$  experimental measurements were reported.  
387 The only comparisons with the system described in this work can be done against flat  
388 panel air-lift PBRs (Chen et al., 2016; Massart et al., 2014). In these works, the authors

389 have used gas for the liquid-biomass mixing, and the reported  $k_{LA}CO_2$  values were higher  
 390 (lower  $CO_2$  solubilization) with respect to the data showed in the present manuscript.

391 **Table 2:** Dependency of  $CO_2$  gas-liquid mass transfer coefficient ( $k_{LA}$ ) on the liquid flow  
 392 velocities and  $CO_2$  flow rates tested.

$k_{LA} CO_2 [s^{-1}]$			
<b>CO<sub>2</sub> flow rate</b> [NL min <sup>-1</sup> ]	<b>Circulator level I *</b> $U_L = 0.17 \text{ m s}^{-1}$	<b>Circulator level II</b> $U_L = 0.60 \text{ m s}^{-1}$	<b>Circulator level III</b> $U_L = 0.77 \text{ m s}^{-1}$
<b>0.06</b>	$1.21 \cdot 10^{-5}$	$1.89 \cdot 10^{-5}$	$1.64 \cdot 10^{-5}$
<b>0.12</b>	$1.47 \cdot 10^{-5}$	$3.43 \cdot 10^{-5}$	$3.20 \cdot 10^{-5}$
<b>0.48</b>	n.d.	$1.30 \cdot 10^{-4}$	$1.24 \cdot 10^{-4}$
<b>1.08</b>	n.d.	n.d.	$2.99 \cdot 10^{-4}$

393 \*  $k_{LA}$  values for level I may be affected by the leak of  $CO_2$  toward the tank (see section [3.1]).

394  
 395 The configuration of the presented PBR applies an innovative liquid handling solution  
 396 that makes difficult to directly compare it with other flat panel PBRs described in  
 397 literature, in terms of hydrodynamics and mass transfer efficiencies. Nevertheless,  
 398 comparisons could be possible by addressing the problem from an energy point of view,  
 399 in terms of energy required per unit volume operating in the unit of time.

400 In the PBR here described, the energy consumption related to the substrate handling  
 401 was evaluated as effective power (at the wall socket) amounting to  $27 \text{ Wh m}^{-3}$  for level II  
 402 of the hydraulic circulator, without any further cost associated to the  $CO_2$  supply and  
 403 stripping-out of  $O_2$ .

404 On the contrary, in the majority of flat panel PBRs described in literature, air is injected  
 405 directly from the bottom of the flat-panels with the triple function of provide adequate  
 406 mixing,  $CO_2$  and favour the stripping-out of  $O_2$ . Therefore, the air supply parameter  
 407 governs the energy consumption and the mass transfer capacity (Leupold et al., 2013;  
 408 Sierra et al., 2008). A large volume of compressed air is therefore consumed to achieve  
 409 the described triple function.

410 A power supply of  $53 \text{ W m}^{-3}$  was estimated by Sierra et al., (2008) to reach a mass  
411 transfer rate high enough to avoid excessive  $\text{O}_2$  accumulation. More recently, Li et al.,  
412 (2014) proposed a new design of flat panel PBR coupled to an external airlift module to  
413 overcome the major limitation of the mixing and improve the energy efficiency of the  
414 process by estimating a power supply of  $31.6 \text{ W m}^{-3}$ . However, the effective energy  
415 consumption of the system must include the efficiency of the associated air compressor,  
416 as also highlighted by Norsker et al., (2012). Therefore, direct comparisons with  
417 traditional flat-panel PBRs are difficult due to the absence of gross energy data  
418 concerning the power consumption of compressed air flat panels.

419

### 420 **3.4 Light homogeneity**

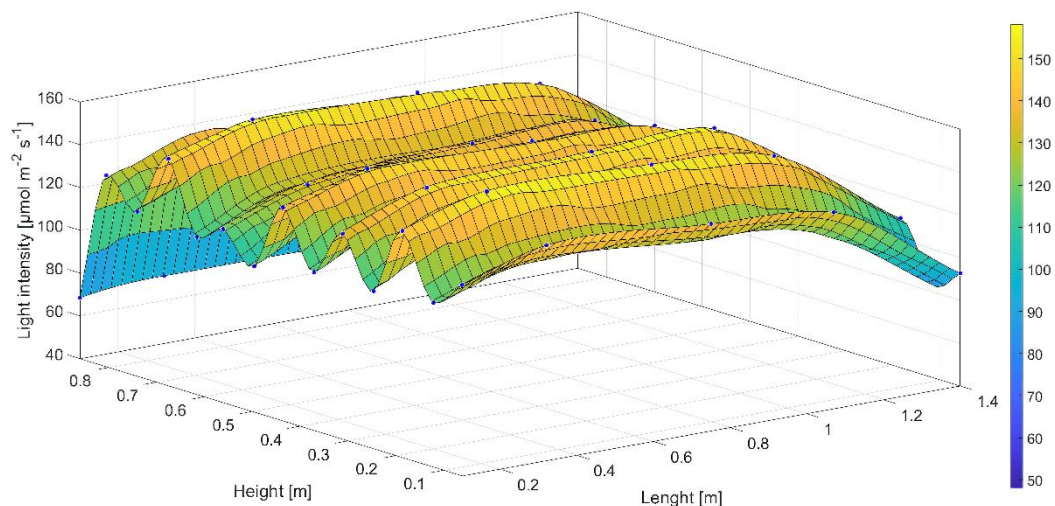
421 The lighting exposure (natural or artificial light) in photoautotrophic cultivation systems  
422 is a major factor influencing the performances of the process. Therefore, in the present  
423 study, we investigated the homogeneity of the artificial lighting system of the PBR  
424 prototype in order to assess the average light intensity at which microalgae cells are  
425 exposed. Light measurements on the surface exposed to the incident light have been used  
426 to build up a radiant matrix [Fig. 4]. The computation of the different measurements on  
427 the surface established a mean incident light intensity of  $120 \mu\text{mol m}^{-2} \text{ s}^{-1}$  with a light  
428 uniformity coefficient  $U_I$  of 40%. The trend of light distribution presents a wave shape,  
429 with the peaks corresponding to the fluorescent tubes positioning along the surface.  
430 Considering the light uniformity coefficient of 40%, a linear liquid velocity of  $0.60 \text{ m s}^{-1}$   
431 (level II), and the length of each alveolus within the flat-panels (around 1.5 m),  
432 microalgae cells take about 10 s to move between two adjacent light intensity peaks.  
433 Therefore, it can be concluded that light fluctuations within the photostage loop do not  
434 significantly affect the overall biomass growth performance.

435 The use of fluorescent tubes as artificial lighting system has some disadvantages.  
436 Fluorescent tubes are omnidirectional light sources, emitting at 360°. Therefore, only half  
437 of the emitted light is directed to the microalgae suspension, whereas the other half might  
438 need to be redirected to the desired area with the use of reflecting surfaces, requiring  
439 additional accessory parts. Moreover, their emitting light intensity, as well as the light  
440 spectrum quality, cannot be tuned if not by increasing the number of tubes (for the light  
441 intensity).

442 The energy consumption of the lighting system, measured as described in section [2.8],  
443 was found to be 455 Wh, a value which must be considered in order to estimate the global  
444 efficiencies of the cultivation system, and to investigate alternative artificial light sources  
445 to overcome the above-reported disadvantages reducing the energy requirements.

446 Further investigations are undergoing to evaluate the implementation of Light Emitting  
447 Diodes (LEDs) as directional light source, due to their overall higher energy efficiency  
448 compared to other commercially available lighting systems.

449



450

451 **Figure 4:** Graphical representation of the light intensity in a 3D space of the fluorescent  
452 source.  $f(x,y)$  = piecewise cubic surface computed with the software Matlab® from p  
453 (structure coefficient), where x is normalized by mean 0.728 and std 0.4788 and where y  
454 is normalized by mean 0.4625 and std 0.2507.

455

### 456 **3.5 Microalgae growth and CO<sub>2</sub> bio-fixation efficiency**

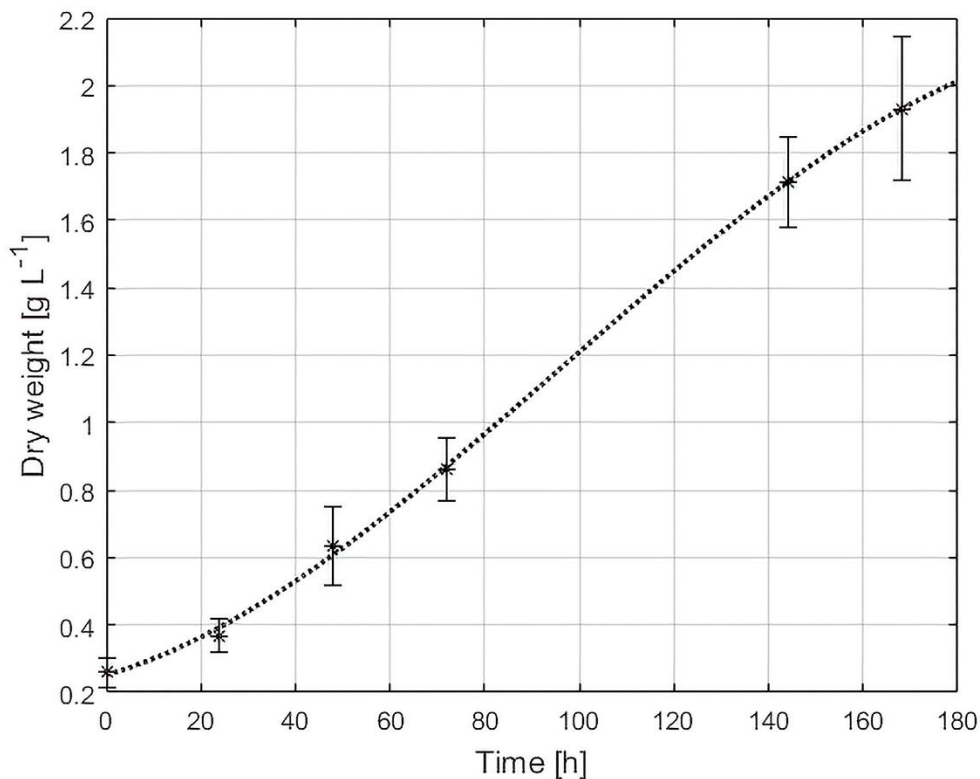
457 Based on the data obtained for what concern the system's hydrodynamics and energy  
458 consumption, it has been decided to assess the growth of the green microalga  
459 *Acutodesmus obliquus* (*Scenedesmus obliquus*) operating at a liquid velocity of 0.60 m s<sup>-1</sup>  
460 (level II) and with a CO<sub>2</sub> flow rate of 0.12 L min<sup>-1</sup>. As mentioned in previous sections,  
461 these hydraulic parameters have been identified among the best performing setups.  
462 Moreover, it has been decided to work at constant dissolved CO<sub>2</sub> concentration of 25 mg  
463 L<sup>-1</sup>, corresponding to a carbon dioxide partial pressure (P<sub>CO<sub>2</sub></sub>) of 0.017 bar. This value has  
464 been chosen to guarantee a relatively high CO<sub>2</sub>/O<sub>2</sub> ratio, which may reduce the potential  
465 negative effects of O<sub>2</sub> accumulation via photorespiration, as suggested by (Sousa et al.,  
466 2012), and to assure a constant control on pH in the range between 7 and 7.5.

467 After 7 days of cultivation the cells reached a final concentration of 1.9 g L<sup>-1</sup> (Fig. 5).  
468 The analysis of the growth curves showed a mean daily volumetric productivity ( $P_x$ ) of  
469 0.21 g L<sup>-1</sup> d<sup>-1</sup> ± 0.01 (n = 3). The CO<sub>2</sub> fixation yield ( $\eta_{CO_2}$ ), calculated as in Eq. 5 and  
470 based on elemental composition analysis of *A. obliquus* previously performed in our  
471 laboratory with the same cultivation setup (C 53.8 %, H 8.88 %, O 37.3% by weight),  
472 accounted for the 64% of the total CO<sub>2</sub> injected.

473 The cultivation of *A. obliquus* was successful in the PBR, and an axenic homogeneous  
474 cell culture could be developed to high cell concentrations. Using fluorescent microscopy,  
475 microalgae cells were found in good shape for the whole batch cultivation (data not  
476 shown), indicating no apparent shear stress despite the use of the mechanical circulating  
477 device set to obtain  $U_L = 0.60$  m s<sup>-1</sup>. Finally, as shown in section [3.2], the average light  
478 intensity on the surface of the flat panels was about 120  $\mu\text{mol m}^{-2} \text{s}^{-1}$ , and the biomass  
479 yield on light energy ranged from 0.3 to 0.6 g mol<sup>-1</sup> during the whole cultivation period,

480 values comparable with data reported for several green microalgae grown in flat panel  
481 reactors (Kliphuis et al., 2010; Li et al., 2014).

482 A recently published review by Lim and co-authors extensively analyzed the CO<sub>2</sub> bio-  
483 fixation results available in literature (Lim et al., 2021). The authors analyzed several  
484 approaches to evaluate the effective CO<sub>2</sub> bio-fixation by microalgae culture and reported  
485 that most of the scientific literature investigated the CO<sub>2</sub> fixation only at laboratory scale.  
486 In this work, for CO<sub>2</sub> bio-fixation calculations we used the elementary analysis approach.  
487 Moreover, the experiments described in this work were performed on volumes higher  
488 than laboratory scale, and additionally a pure CO<sub>2</sub> stream was used to feed the PBR in a  
489 way that could be compatible with already available industrial streams. The obtained  
490 results place the new flat-panel PBR among the most promising prototypal technology to  
491 implement a microalgae CO<sub>2</sub> fixation approach at industrial scale. Furthermore, the  
492 hardware components of the PBR, equipped with a multi-probes system connected via  
493 transducer to an integrated PLC (see section [2.1]), make this pilot-scale prototype  
494 already suitable for remote monitoring and control of cultivation parameters to  
495 incorporate the Internet of Things (IoT). This, as extensively highlighted in recent  
496 literature, is becoming a relevant aspect as both academic research and industry are  
497 gradually moving towards process automation and remote operation (Tham et al., 2022;  
498 Wang et al., 2022).



499

500 **Figure 5:** Biomass concentration of *Acutodesmus obliquus* in the flat panel  
 501 photobioreactor. Stars represent the dry weight measurements  $\pm$  standard deviation ( $n =$   
 502 3). Dotted line represents the third-degree polynomial interpolation ( $R^2 = 0.9985$ )  
 503 obtained with the software Matlab®.

504

#### 505 4. Conclusion

506 This study provides the characterization of a new flat panel PBR prototype regarding  
 507 the main hydrodynamic parameters, the CO<sub>2</sub> supply strategy and the artificial lighting  
 508 system. An innovative liquid handling strategy based on a pump-assisted circulation has  
 509 been proposed and tested in this work. The liquid culture is moved by a centrifugal pump  
 510 that allows to achieve appropriate culture mixing and enhance CO<sub>2</sub> mass transfer with a  
 511 lower power consumption compared to the majority of flat-panels described in the  
 512 literature. The biological performances of the system have been successfully tested by  
 513 cultivating the green microalgae *Acutodesmus obliquus*, which showed a mean daily  
 514 volumetric productivity ( $P_v$ ) of 0.21 g L<sup>-1</sup> d<sup>-1</sup> and a biomass yield on light energy  
 515 comparable to those reported for several green microalgae in flat-panel PBRs.



516 Furthermore, the CO<sub>2</sub> bio-fixation efficiency was found to be higher (64%) than those  
517 reported in literature for several microalgae species grown in large-scale setups. Taken  
518 all together, the energetic and biological performances of this pilot-scale PBR may  
519 constitute an important step toward the development of industrial-scale technologies to  
520 mitigate CO<sub>2</sub> while obtaining high quality microalgal biomass. Future work will be  
521 carried out in order to further reduce the energy consumption, optimize CO<sub>2</sub> and light  
522 supply strategies, as well as several other cultivation parameters (e.g., media composition,  
523 temperature, light quality), to further optimize the overall photobioreactor CapEx and  
524 OpEx.

525

#### 526 **Declaration of Competing Interest**

527 The authors declare that the research was conducted in the absence of any commercial or  
528 financial relationships that could be construed as a potential conflict of interest.

529

#### 530 **Acknowledgements**

531 This work was supported by Politecnico di Torino and the Wearwe group @PoliTo  
532 (58\_DIM21RIGVIN; 58\_RCE19ZANMAR\_03). The authors are grateful to Arcobaleno  
533 Cooperativa Sociale (Torino, Italy) in the person of F. Passarelli and F. De Bernardi for  
534 their technical support.

535

#### 536 **Author contributions**

537 M.C., A.O., M.Z. and V.A.R. designed research; M.C., D.A., V.C., and C.D. performed  
538 research; M.C. and V.C. analysed data; M.C. and V.A.R. wrote the article.

539

540

541

542 **References**

- 543 Acién, F.G., Fernández, J.M., Magán, J.J., Molina, E., 2012. Production cost of a real  
544 microalgae production plant and strategies to reduce it. *Biotechnology*  
545 *Advances* 30, 1344–1353.  
546 <https://doi.org/10.1016/j.biotechadv.2012.02.005>
- 547 Acién, F.G., Molina, E., Reis, A., Torzillo, G., Zittelli, G.C., Sepúlveda, C., Masojídek,  
548 J., 2017. Photobioreactors for the production of microalgae, *Microalgae-*  
549 *Based Biofuels and Bioproducts: From Feedstock Cultivation to End-*  
550 *Products.* <https://doi.org/10.1016/B978-0-08-101023-5.00001-7>
- 551 Adesanya, V.O., Cadena, E., Scott, S.A., Smith, A.G., 2014. Life cycle assessment on  
552 microalgal biodiesel production using a hybrid cultivation system.  
553 *Bioresource Technology* 163, 343–355.  
554 <https://doi.org/10.1016/j.biortech.2014.04.051>
- 555 Benemann, J., 2013. Microalgae for biofuels and animal feeds. *Energies (Basel)* 6,  
556 5869–5886. <https://doi.org/10.3390/en6115869>
- 557 Blunden, J., Boyer, T., 2021. State of the climate in 2020. *Bull Am Meteorol Soc.*  
558 <https://doi.org/10.1175/2021BAMSStateoftheClimate.1>
- 559 Brown, L.M., Zeiler, K.G., 1993. Aquatic biomass and carbon dioxide trapping.  
560 *Energy Conversion and Management* 34, 1005–1013.  
561 [https://doi.org/10.1016/0196-8904\(93\)90048-F](https://doi.org/10.1016/0196-8904(93)90048-F)
- 562 Carlsson, A.S., van Beilen, J.B., Möller, R., Clayton, D., 2007. *Micro- and Macro-*  
563 *algae: Utility for Industrial Applications. Outputs from the EPOBIO Project.*  
564 CPL Press, Berks.
- 565 Carvalho, A.P., Meireles, L.A., Malcata, F.X., 2006. Microalgal Reactors: A Review  
566 of Enclosed System Designs and Performances. *Biotechnol Prog* 22, 1490–  
567 1506. <https://doi.org/10.1021/bp060065r>

568 Cheah, W.Y., Show, P.L., Chang, J.S., Ling, T.C., Juan, J.C., 2015. Biosequestration of  
569 atmospheric CO<sub>2</sub> and flue gas-containing CO<sub>2</sub> by microalgae. *Bioresource*  
570 *Technology* 184, 190–201. <https://doi.org/10.1016/j.biortech.2014.11.026>

571 Chen, Z., Jiang, Z., Zhang, X., Zhang, J., 2016. Numerical and experimental study on  
572 the CO<sub>2</sub> gas-liquid mass transfer in flat-plate airlift photobioreactor with  
573 different baffles. *Biochemical Engineering Journal* 106, 129–138.  
574 <https://doi.org/10.1016/j.bej.2015.11.011>

575 Chiaramonti, D., Prussi, M., Casini, D., Tredici, M.R., Rodolfi, L., Bassi, N., Zittelli,  
576 G.C., Bondioli, P., 2013. Review of energy balance in raceway ponds for  
577 microalgae cultivation: Re-thinking a traditional system is possible. *Applied*  
578 *Energy* 102, 101–111. <https://doi.org/10.1016/j.apenergy.2012.07.040>

579 Chini Zittelli, G., Rodolfi, L., Bassi, N., Biondi, N., Tredici, M.R., 2013.  
580 Photobioreactors for microalgae biofuel production, in: Borowitzka, M.A.,  
581 Moheimani, N.R. (Eds.), *Algae for Biofuels and Energy*. Springer, Dodrecht.,  
582 pp. 115–131. <https://doi.org/10.1007/978-94-007-5479-9>

583 Chisti, Y.M., 1989. *Airlift Bioreactors*. Elsevier, London.

584 Cuaresma, M., Janssen, M., Vílchez, C., Wijffels, R.H., 2009. Productivity of *Chlorella*  
585 *sorokiniana* in a short light-path (SLP) panel photobioreactor under high  
586 irradiance. *Biotechnology and Bioengineering* 104, 352–359.  
587 <https://doi.org/10.1002/bit.22394>

588 De Vree, J.H., Bosma, R., Janssen, M., Barbosa, M.J., Wijffels, R.H., 2015. Comparison  
589 of four outdoor pilot-scale photobioreactors. *Biotechnology for Biofuels* 8,  
590 1–12. <https://doi.org/10.1186/s13068-015-0400-2>

591 del Rio-Chanona, E.A., Wagner, J.L., Ali, H., Fiorelli, F., Zhang, D., Hellgardt, K., 2019.  
592 Deep learning-based surrogate modeling and optimization for microalgal  
593 biofuel production and photobioreactor design. *AIChE Journal* 65, 915–923.  
594 <https://doi.org/10.1002/aic.16473>

595 Estrada-Graf, A., Hernández, S., Morales, M., 2020. Biomitigation of CO<sub>2</sub> from flue  
596 gas by *Scenedesmus obtusiusculus* AT-UAM using a hybrid photobioreactor  
597 coupled to a biomass recovery stage by electro-coagulation-flotation.  
598 *Environmental Science and Pollution Research*.  
599 <https://doi.org/10.1007/s11356-020-08240-2>

600 Francisco, É.C., Neves, D.B., Jacob-Lopes, E., Franco, T.T., 2010. Microalgae as  
601 feedstock for biodiesel production: Carbon dioxide sequestration, lipid  
602 production and biofuel quality. *Journal of Chemical Technology and  
603 Biotechnology* 85, 395–403. <https://doi.org/10.1002/jctb.2338>

604 Gimpel, J.A., Henríquez, V., Mayfield, S.P., 2015. In metabolic engineering of  
605 eukaryotic microalgae: Potential and challenges come with great diversity.  
606 *Frontiers in Microbiology* 6, 1–14.  
607 <https://doi.org/10.3389/fmicb.2015.01376>

608 Goli, A., Shamiri, A., Talaiekhosani, A., Eshtiaghi, N., Aghamohammadi, N., Aroua,  
609 M.K., 2016. An overview of biological processes and their potential for CO<sub>2</sub>  
610 capture. *Journal of Environmental Management*.  
611 <https://doi.org/10.1016/j.jenvman.2016.08.054>

612 Greenwell, H.C., Laurens, L.M.L., Shields, R.J., Lovitt, R.W., Flynn, K.J., 2010. Placing  
613 microalgae on the biofuels priority list: A review of the technological  
614 challenges. *Journal of the Royal Society Interface* 7, 703–726.  
615 <https://doi.org/10.1098/rsif.2009.0322>

616 Jorquera, O., Kiperstok, A., Sales, E.A., Embiruçu, M., Ghirardi, M.L., 2010.  
617 Comparative energy life-cycle analyses of microalgal biomass production in  
618 open ponds and photobioreactors. *Bioresource Technology* 101, 1406–  
619 1413. <https://doi.org/10.1016/j.biortech.2009.09.038>

620 Khan, S.A., Rashmi, Hussain, M.Z., Prasad, S., Banerjee, U.C., 2009. Prospects of  
621 biodiesel production from microalgae in India. *Renewable and Sustainable*

622 Energy Reviews 13, 2361–2372.  
623 <https://doi.org/10.1016/j.rser.2009.04.005>

624 Kliphuis, A.M.J., de Winter, L., Vejrazka, C., Martens, D.E., Janssen, M., Wijffels, R.H.,  
625 2010. Photosynthetic efficiency of *Chlorella sorokiniana* in a turbulently  
626 mixed short light-path photobioreactor. *Biotechnology Progress* 26, 687–  
627 696. <https://doi.org/10.1002/btpr.379>

628 Leupold, M., Hindersin, S., Kerner, M., Hanelt, D., 2013. The effect of discontinuous  
629 airlift mixing in outdoor flat panel photobioreactors on growth of  
630 *Scenedesmus obliquus*. *Bioprocess and Biosystems Engineering* 36, 1653–  
631 1663. <https://doi.org/10.1007/s00449-013-0939-x>

632 Li, J., Stamato, M., Velliou, E., Jeffryes, C., Agathos, S.N., 2014. Design and  
633 characterization of a scalable airlift flat panel photobioreactor for  
634 microalgae cultivation. *Journal of Applied Phycology* 27, 75–86.  
635 <https://doi.org/10.1007/s10811-014-0335-1>

636 Lim, Y.A., Chong, M.N., Foo, S.C., Ilankoon, I.M.S.K., 2021. Analysis of direct and  
637 indirect quantification methods of CO<sub>2</sub> fixation via microalgae cultivation in  
638 photobioreactors: A critical review. *Renewable and Sustainable Energy*  
639 *Reviews* 137, 110579. <https://doi.org/10.1016/j.rser.2020.110579>

640 López-Rosales, L., Sánchez-Mirón, A., Contreras-Gómez, A., García-Camacho, F.,  
641 Battaglia, F., Zhao, L., Molina-Grima, E., 2019. Characterization of bubble  
642 column photobioreactors for shear-sensitive microalgae culture.  
643 *Bioresource Technology* 275, 1–9.  
644 <https://doi.org/10.1016/j.biortech.2018.12.009>

645 Massart, A., Mirisola, A., Lupant, D., Thomas, D., Hantson, A.L., 2014. Experimental  
646 characterization and numerical simulation of the hydrodynamics in an airlift  
647 photobioreactor for microalgae cultures. *Algal Research* 6, 210–217.  
648 <https://doi.org/10.1016/j.algal.2014.07.003>

649 Norsker, H., Barbosa, M.J., Vermuë, M.H., Wijffels, R.H., 2012. On Energy Balance  
650 and Production Costs in Tubular and Flat Panel Photobioreactors. *TATuP -*  
651 *Zeitschrift für Technikfolgenabschätzung in Theorie und Praxis* 21, 54–62.  
652 <https://doi.org/10.14512/tatup.21.1.54>

653 Norsker, N.H., Barbosa, M.J., Vermuë, M.H., Wijffels, R.H., 2011. Microalgal  
654 production - A close look at the economics. *Biotechnology Advances* 29, 24–  
655 27. <https://doi.org/10.1016/j.biotechadv.2010.08.005>

656 Pandey, A., Lee, D.J., Chisti, Y., Soccol, C.R., 2014. *Biofuels From Algae* Biofuels  
657 From. Elsevier, Amsterdam.

658 Perin, G., Simionato, D., Bellan, A., Carone, M., Occhipinti, A., Maffei, M.E.,  
659 Morosinotto, T., 2017. Cultivation in industrially relevant conditions has a  
660 strong influence on biological properties and performances of  
661 *Nannochloropsis gaditana* genetically modified strains. *Algal Research* 28,  
662 88–99. <https://doi.org/10.1016/j.algal.2017.10.013>

663 Reyna-Velarde, R., Cristiani-Urbina, E., Hernández-Melchor, D.J., Thalasso, F.,  
664 Cañizares-Villanueva, R.O., 2010. Hydrodynamic and mass transfer  
665 characterization of a flat-panel airlift photobioreactor with high light path.  
666 *Chemical Engineering and Processing: Process Intensification* 49, 97–103.  
667 <https://doi.org/10.1016/j.cep.2009.11.014>

668 Rodolfi, L., Zittelli, G.C., Bassi, N., Padovani, G., Biondi, N., Bonini, G., Tredici, M.R.,  
669 2009. Microalgae for oil: Strain selection, induction of lipid synthesis and  
670 outdoor mass cultivation in a low-cost photobioreactor. *Biotechnology and*  
671 *Bioengineering* 102, 100–112. <https://doi.org/10.1002/bit.22033>

672 Rosenberg, J.N., Mathias, A., Korth, K., Betenbaugh, M.J., Oyler, G.A., 2011.  
673 Microalgal biomass production and carbon dioxide sequestration from an  
674 integrated ethanol biorefinery in Iowa: A technical appraisal and economic  
675 feasibility evaluation. *Biomass and Bioenergy* 35, 3865–3876.  
676 <https://doi.org/10.1016/j.biombioe.2011.05.014>

677 Sierra, E., Ación, F.G., Fernández, J.M., García, J.L., González, C., Molina, E., 2008.  
678 Characterization of a flat plate photobioreactor for the production of  
679 microalgae. *Chemical Engineering Journal* 138, 136–147.  
680 <https://doi.org/10.1016/j.cej.2007.06.004>

681 Slade, R., Bauen, A., 2013. Micro-algae cultivation for biofuels: Cost, energy  
682 balance, environmental impacts and future prospects. *Biomass and  
683 Bioenergy* 53, 29–38. <https://doi.org/10.1016/j.biombioe.2012.12.019>

684 Solimeno, A., Gabriel, F., García, J., 2017. Mechanistic model for design, analysis,  
685 operation and control of microalgae cultures: Calibration and application to  
686 tubular photobioreactors. *Algal Research* 21, 236–246.  
687 <https://doi.org/10.1016/j.algal.2016.11.023>

688 Sousa, C., de Winter, L., Janssen, M., Vermuë, M.H., Wijffels, R.H., 2012. Growth of  
689 the microalgae *Neochloris oleoabundans* at high partial oxygen pressures  
690 and sub-saturating light intensity. *Bioresource Technology* 104, 565–570.  
691 <https://doi.org/10.1016/j.biortech.2011.10.048>

692 Stanier, R.Y., Kunisawa, R., Mandel, M., Cohen-Bazire, G., 1971. Purification and  
693 properties of unicellular blue-green algae (order Chroococcales). *Bacteriol  
694 Rev* 35, 171–205. <https://doi.org/10.1128/membr.35.2.171-205.1971>

695 Tan, C.H., Tan, X., Ho, S.H., Lam, S.S., Show, P.L., Nguyen, T.H.P., 2020. Conceptual  
696 design of a hybrid thin layer cascade photobioreactor for microalgal  
697 biodiesel synthesis. *International Journal of Energy Research* 44, 9757–  
698 9771. <https://doi.org/10.1002/er.5699>

699 Tham, P.E., Ng, Y.J., Vadivelu, N., Lim, H.R., Khoo, K.S., Chew, K.W., Show, P.L., 2022.  
700 Sustainable smart photobioreactor for continuous cultivation of microalgae  
701 embedded with Internet of Things. *Bioresource Technology* 346.  
702 <https://doi.org/10.1016/j.biortech.2021.126558>

703 Torzillo, G., Pushparaj, B., Masojidek, J., Vonshak, A., 2003. Biological constraints  
704 in algal biotechnology. *Biotechnology and Bioprocess Engineering* 8, 338–  
705 348. <https://doi.org/10.1007/BF02949277>

706 Torzillo, G., Zittelli, G.C., 2015. Tubular Photobioreactors, in: Prokop, A., Bajpai,  
707 R.K., Zappi, M.E. (Eds.), *Algal Biorefineries. In: Products and Refinery Design*,  
708 Vol. 2. Springer, Switzerland, pp. 187–212. <https://doi.org/10.1007/978-3-319-20200-6>

709

710 Tredici, M.R., Bassi, N., Prussi, M., Biondi, N., Rodolfi, L., Chini Zittelli, G.,  
711 Sampietro, G., 2015. Energy balance of algal biomass production in a 1-ha  
712 “Green Wall Panel” plant: How to produce algal biomass in a closed reactor  
713 achieving a high Net Energy Ratio. *Applied Energy* 154, 1103–1111.  
714 <https://doi.org/10.1016/j.apenergy.2015.01.086>

715 Tredici, M.R., Chini Zittelli, G., Rodolfi, L., 2010. Photobioreactors, in: Flickinger,  
716 M.C. (Ed.), *Encyclopedia of Industrial Biotechnology: Bioprocess,*  
717 *Bioseparation, and Cell Technol- Ogy.* Wiley, Hoboken, NJ, pp. 3821–3838.  
718 <https://doi.org/10.1002/9780470054581.eib479>

719 Vanthoor-Koopmans, M., Wijffels, R.H., Barbosa, M.J., Eppink, M.H.M., 2013.  
720 Biorefinery of microalgae for food and fuel. *Bioresource Technology* 135,  
721 142–149. <https://doi.org/10.1016/j.biortech.2012.10.135>

722 Vasile, N.S., Cordara, A., Usai, G., Re, A., 2021. Computational analysis of dynamic  
723 light exposure of unicellular algal cells in a flat-panel photobioreactor to  
724 support light-induced CO<sub>2</sub> bioprocess development. *Frontiers in*  
725 *Microbiology* 12. <https://doi.org/10.3389/fmicb.2021.639482>

726 Wang, K., Khoo, K.S., Leong, H.Y., Nagarajan, D., Chew, K.W., Ting, H.Y., Selvarajoo,  
727 A., Chang, J.S., Show, P.L., 2022. How does the Internet of Things (IoT) help  
728 in microalgae biorefinery? *Biotechnology Advances.*  
729 <https://doi.org/10.1016/j.biotechadv.2021.107819>



730           Weise, T., Reinecke, J.M., Schuster, S., Pfaff, M., 2019. Optimizing turbidostatic  
731           microalgal biomass productivity: A combined experimental and coarse-  
732           grained modelling approach. *Algal Research* 39.  
733           <https://doi.org/10.1016/j.algal.2019.101439>

734           Yadav, G., Karemore, A., Dash, S.K., Sen, R., 2015. Performance evaluation of a  
735           green process for microalgal CO<sub>2</sub> sequestration in closed photobioreactor  
736           using flue gas generated in-situ. *Bioresource Technology* 191, 399–406.  
737           <https://doi.org/10.1016/j.biortech.2015.04.040>

738           Yadav, G., Sen, R., 2017. Microalgal green refinery concept for biosequestration of  
739           carbon-dioxide vis-à-vis wastewater remediation and bioenergy  
740           production: Recent technological advances in climate research. *Journal of*  
741           *CO<sub>2</sub> Utilization* 17, 188–206. <https://doi.org/10.1016/j.jcou.2016.12.006>

742           Yang, C., Mao, Z.-S., 2014. Airlift loop reactors, in: Yang, C., Zai-Sha, M. (Eds.),  
743           *Numerical Simulation of Multiphase Reactors with Continuous Liquid Phase*.  
744           pp. 153–229. <https://doi.org/10.1016/b978-0-08-099919-7.00004-4>

745